

MODELING AND PARAMETRIC STUDIES OF HEAT TRANSFER IN A TUBULAR METHANE-STEAM REFORMER WITH A CONVECTION-RADIATION CONVERTER

SUMRERNG JUGJAI

*Department of Mechanical Engineering
King Mongkut's Institute of Technology Thonburi
Bangkok 10140*

ABSTRACT

A mathematical system model of a two-dimensional tubular methane steam reformer with a convection-radiation converter (porous medium) has been developed. Mixture of methane and steam flowing inside a reacting pipe travels counterflow to the combustion gas flowing in a furnace of the reformer. The reformer is modeled by means of a proposed quasi-multidimensional analytical model, in which a two-dimensional energy equation is integrated and averaged along the direction perpendicular to the flow of the combustion gas. The divergence of radiation for a participating gas is also averaged after the rigorous three-dimensional treatment relating to the radiative transfer. An extensive parametric investigation has been completed to determine the operating characteristics of the reformer. The parametric investigations included in this paper study the effect of absorption coefficient of the combustion gas, the flow velocity of the combustion gas, the flow velocity of the methane-steam mixture and the type of the reformer head (porous medium or insulated wall).

1. INTRODUCTION

Heat transfer in a preheating furnace is so complicated that the heat transfer analysis with a satisfactory degree of accuracy could not be easily done. This is because the heat transfer process in the furnace includes many complicated factors such as radiation which occupies a main portion of the processes, type of furnace, furnace configuration as well as flame shape. Many methods concerning the analysis of this heat transfer have been proposed such as a simple gas lump model, Monte Carlo method, zoning method, two-flux model and multi-flux model. Besides, for the limiting cases as the optical length of the reacting gas become thick or thin, the Rosseland approximation and transparent approximation(1), respectively, are suitable methods. Since each method has its own special feature, it is necessary to select the most appropriate method that will comply with the required answer. Numerous computer codes have come into wide use in designing a furnace or assessment of the heat transfer characteristics of a specific problem. However, accuracy of the solution is still controversial in many cases.

In this paper, a quasi-multi-dimensional analytical model has been proposed for a

two-dimensional tubular methane-steam reformer, the combustion chamber of which is equipped with a convection-radiation converter (porous medium). The model is relatively convenient with a high accurate output. The radiative properties of the reacting gas are considered in the model and the results of the heat transfer analysis are reported.

2. TUBULAR HEATING FURNACE WITH CONVECTION-RADIATION CONVERTER

In general, tubular heating furnaces with various configurations and special features are widely made in practical use. On the other hand, the porous medium technology can be suitably applied successfully to the heating furnaces (2,3,4). Figure 1 exhibits a typical methane-steam reformer equipped with the porous medium. The combustion gas produced by burners at the furnace floor flow upwards through the porous medium and then flows out of the furnace at the top end. Meanwhile, the reacting pipe walls located between two burners are heated by the radiative energy emitted from the combustion gas and from the porous medium.

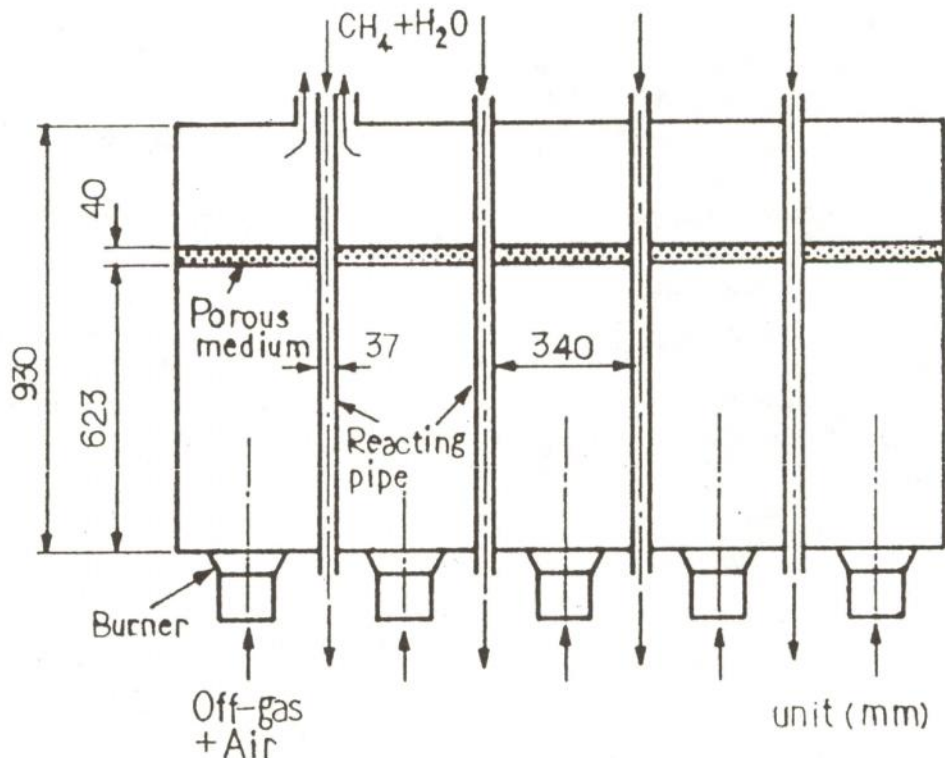


Fig. 1 Methane-steam reformer equipped with porous medium.

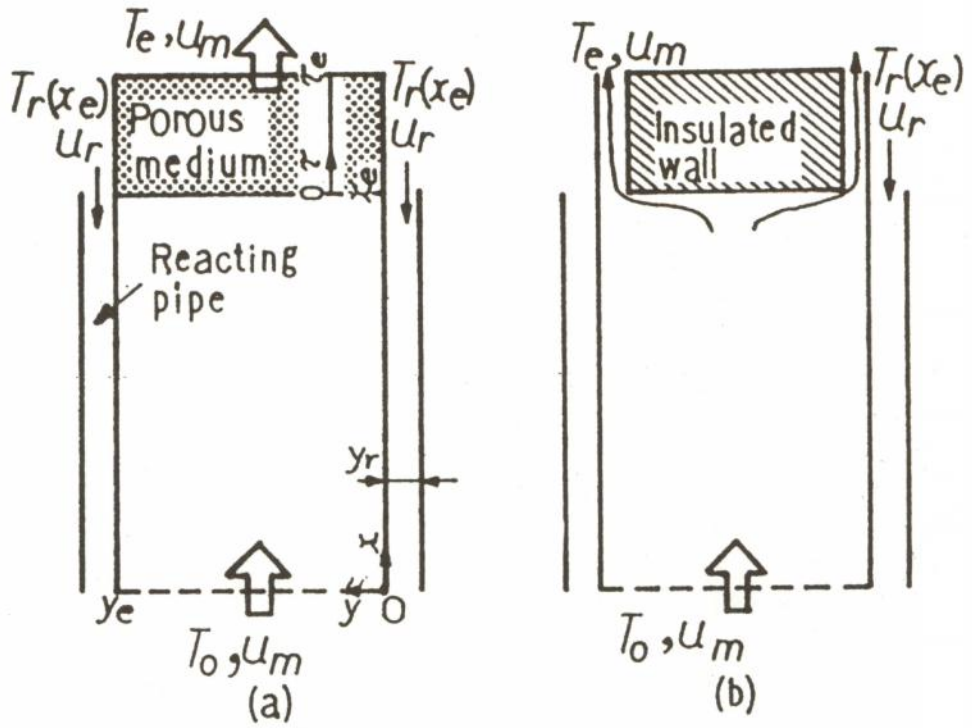


Fig. 2 Physical model (a) porous medium (b) insulated wall.

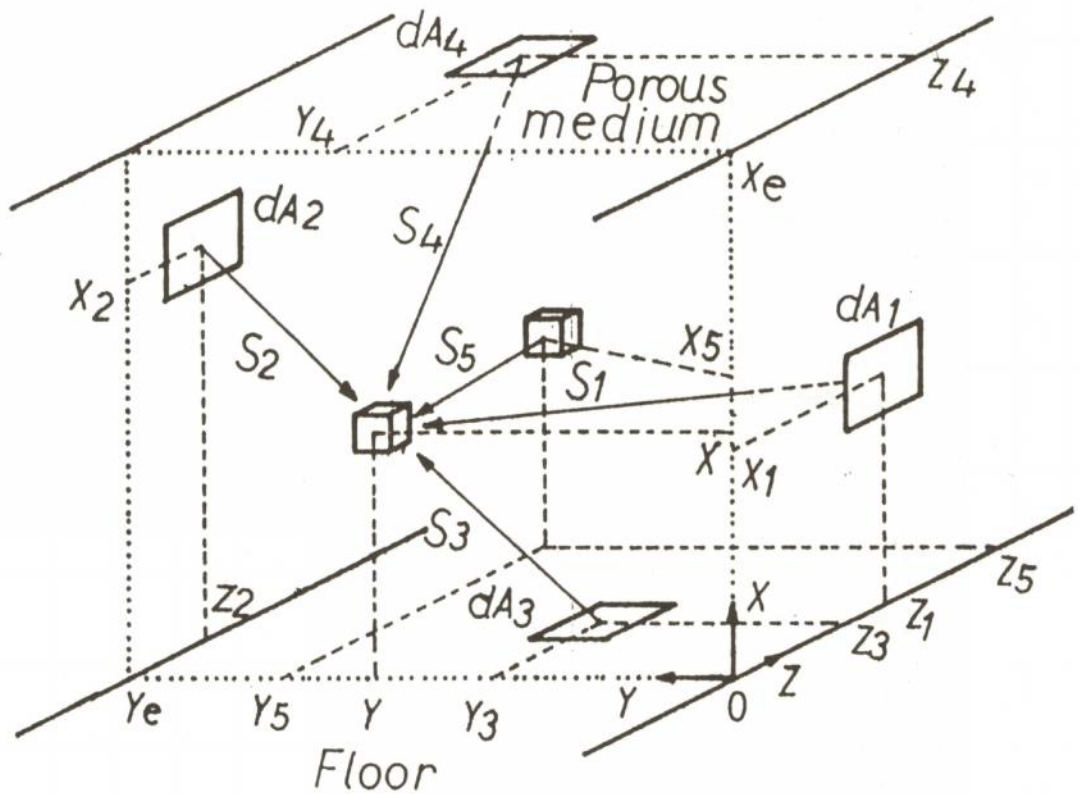


Fig. 3 Radiative heat transfer from each emitter to gas volume element.

3. THEORETICAL ANALYSIS

3.1 Analytical model

Figures 2(a) and 2(b) illustrate an analytical model of one segment for the heat transfer system as shown in Fig. 1. The indefinite z direction which is perpendicular to the plane of the paper characterizes a two dimensional flow path of the system. The structural walls of the system are specified as follows: insulated wall for the floor, heat extraction walls for the two side walls, and porous medium (Fig.2 (a)) or insulated wall (Fig. 2 (b)) for the ceiling. Working gas (either participating or nonparticipating medium) at high temperature T_o and uniform velocity u_m enters the system through the floor and flows into the porous medium or a narrow path between the insulated wall and the heat extraction wall and then exhausts to the outer at the upper end. On the other hand, a mixture of methane and steam flows downwards inside the reacting pipe in which endothermic reaction (based on the Arrhenius-type reaction rate) due to reforming reaction is taking place. The reacting pipe can be simply considered as a water-cooled or air-cooled wall of the system.

The major assumptions upon which the present model is based are:

1. The porous medium consists of very fine particles which is uniformly distributed.
2. The gas and the porous medium are considered as gray body which is capable of absorbing and emitting thermal radiation.
3. Radiative heat transfer inside the porous medium is approximated as one dimension along the flow direction and the radiation of gas is negligible as compared to that of the solid.
4. The heat extraction wall is assumed black and its resistance of heat transfer is negligible.
5. Physical properties are constant.

3.2 Governing equations

Base on the above mentioned assumptions and the general three dimensional energy equation in which convection, conduction and radiation are taken into consideration inside the furnace under steady state condition can be expressed as

$$\rho C_p (u \frac{\partial T}{\partial x} + v \frac{\partial T}{\partial y} + w \frac{\partial T}{\partial z}) = \lambda (\frac{\partial^2 T}{\partial x^2} + \frac{\partial^2 T}{\partial y^2} + \frac{\partial^2 T}{\partial z^2}) - \text{div } \bar{q}_r \quad (1)$$

since the considered system is characterized as a two-dimensional flow path, the equation (1) can be integrated and averaged along the y direction and becomes

$$\rho C_p u_m \frac{dT_m}{dx} = \lambda \frac{d^2 T_m}{dx^2} - \frac{2h_m}{y_e} (T_m - T_w) - \frac{1}{y_e} \int_0^{y_e} [\text{div } \bar{q}_r] dy \quad (2)$$

where h_m is heat transfer coefficient at the heat extraction wall (furnace side).

The divergence of the net radiative heat flux is a function of optical distance S_1 to S_5 as shown in Fig. 3 and is expressed as

$$\begin{aligned} & - \text{div } \bar{q}_r \\ & = \kappa_g \frac{\sigma}{\pi} \int_0^{x_e} T_w^4(x') \int_{-\infty}^{\infty} \frac{\exp(-\kappa_g S_1)}{S_1^3} y dz' dx' \\ & \quad + \kappa_g \frac{\sigma}{\pi} \int_0^{x_e} T_w^4(x') \int_{-\infty}^{\infty} \frac{\exp(-\kappa_g S_2)}{S_2^3} (y_e - y) dz' dx' \\ & \quad + \kappa_g \frac{\sigma}{\pi} T_f^4 \int_{-y_e}^0 \int_{-\infty}^{\infty} \frac{\exp(-\kappa_g S_3)}{S_3^3} x dz' dy' \\ & \quad + \kappa_g \frac{\sigma}{\pi} T_m^4 \int_0^{y_e} \int_{-\infty}^{\infty} \frac{\exp(-\kappa_g S_4)}{S_4^3} (x_e - x) dz' dy' \\ & \quad + \kappa_g^2 \frac{\sigma}{\pi} \int_0^{x_e} T_m^4(x') \int_0^{y_e} \int_{-\infty}^{\infty} \frac{\exp(-\kappa_g S_5)}{S_5^3} dz' dy' dx' \\ & \quad - 4 \kappa_g \sigma T_m^4(x) \end{aligned} \quad (3)$$

where $T_w(x)$, $T_m(x)$, T_f and T_{pe} , respectively, represent temperatures of the heat extraction wall, average temperature of gas along the y direction, temperature of the insulated floor and temperature of a black body which has an equivalent radiative heat flux to that emitted from the porous medium ($\sigma T_{pe}^4 = q_{rp}^-(0)$; $q_{rp}^-(0)$ is calculated from Eq. (7)). By one dimensional approximation of the thermal radiation propagation inside the porous medium, the basic equations for this region can be written as (5)

$$\rho C_p u_m \frac{dT_m}{dx} = \lambda \frac{d^2 T_m}{dx^2} - h_p n_p A_p (T_m - T_p) \quad (4)$$

solid phase (porous medium):

$$h_p n_p A_p (T_m - T_p) - \frac{dq_{rp}}{dx} = 0 \quad (5)$$

The forward, backward and net radiative heat flux in the porous medium can be expressed as

$$q_{rp}(\tau) = 2\pi [I_{pe,m} E_3(\tau) + \int_0^\tau I_b(\tau') E_2(\tau - \tau') d\tau'] \quad (6)$$

$$q_{rp}^-(\tau) = -2\pi [I_b E_3(\tau_e - \tau) + \int_\tau^{\tau_e} I_b(\tau') E_2(\tau' - \tau) d\tau'] \quad (7)$$

$$q_{rp}(\tau) = q_{rp}^+(\tau) + q_{rp}^-(\tau) \quad (8)$$

where $I_{pe,m}$, I_e and $E_n(\tau)$, respectively, represent averaged incidence radiation intensity from the furnace along the x direction on the upstream surface of the porous medium, incidence radiation intensity from a downstream black body at an equivalent temperature to that of the downstream surface of the porous medium and exponential integral function.

Taking the absorption of radiation by the working gas into consideration, the radiative heat exchange between structural walls could be written in the same manner as Eq. (3). In this case, the porous medium is treated as a black body surface at temperature of T_{pe} . On the other hand, for the case of the insulated wall (Fig. 2(b)), its temperature is calculated by assuming that the radiative heat flux emitted from it is equal to the summation of the incidence radiative heat flux and the convective heat flux at the surface.

Assuming that the endothermic reaction of methane and steam in the reacting pipe is one-step global reaction given by the Arrhenius law, the product species conservation equation and the energy equation can be written as

$$\rho_r u_r \frac{dy}{dx} = A \rho_r (1 - y) \exp\left(-\frac{E}{RT_r}\right) \quad (9)$$

$$\rho_r C_p u_r \frac{dT_r}{dx} = \frac{2h_r}{y_r} (T_w - T_r) - A \rho_r h_0 (1 - y) \exp\left(-\frac{E}{RT_r}\right) \quad (10)$$

The temperature of the heat extraction wall at any x location can be calculated from the equality of the heat flux at the furnace side and the reacting pipe side as

$$2h_r (T_w - T_r) = 2q_n(x) + 2h_m (T_m - T_w) \quad (11)$$

where h_r is heat transfer coefficient at the heat extraction wall (reacting pipe side).

3.3 Approximate analysis method

Equation (2) to (11) are solved simultaneously. It is necessary to treat the radiation term (Eq. (3)) as a three dimensional problem. First, the attenuation part of the equation is integrated along the z direction up to the range at which the accuracy of the integration being maintained. As shown in Fig. 4, when considering the incidence radiative energy from a gas volume element at position (x' , y') on another gas volume at position (x , y), the shape factor from the gas volume element at each y' position on any location of x' to the element at position (x , y) can be computed in advance and excluded from the iterative computation, since the average gas temperature $T_m(x')$ is employed. As a consequence, the divergence of the net radiative heat flux at each y position on any location of x can be obtained and is averaged along the y direction. Then the temperature distribution in the furnace which could be considered as a quasi-multi-dimensional problem is computed from Eq. 2. However, singularity points yield in the process of integration for the radiation term. As a result, the integrand at the point can be estimated by extrapolation of the two adjacent points.

The number of mesh used in the computation is 10 for both x and y direction of the furnace, 40 for the porous medium and 10 for the reacting pipe. Since there is a possibility of sharp temperature gradient occurring inside the furnace in the vicinity of the porous medium, an imaginary region of the same thickness as that of the porous medium is established so as to yield a smooth connection of the temperature distribution

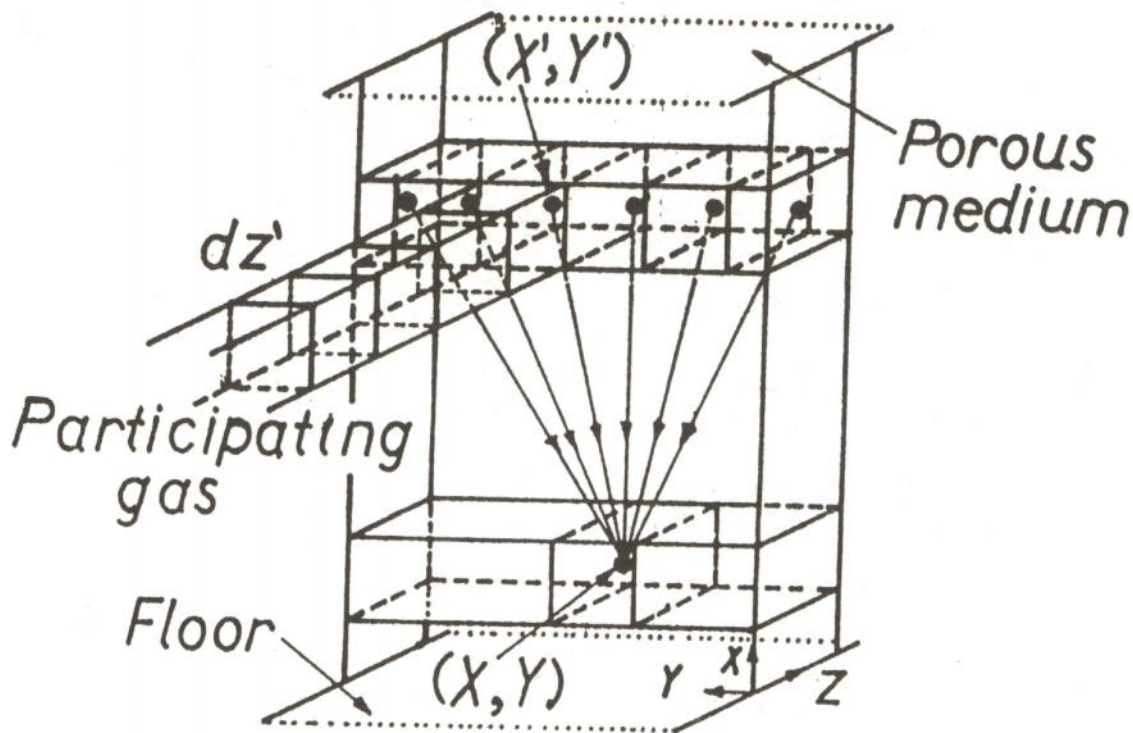


Fig. 4 Radiative heat transfer between gas volume elements.

in the region. In this region, only convection and conduction are considered and the number of mesh used is 10.

The necessary values used in the computation are based on the experimental parameters of the equipment shown in Fig. 1 and the main important values are listed in Table 1.

TABLE 1.

Values of Various Parameter Used in the Tubular Methane-Steam Reformer

Parameters	Values
T_o	(Furnace inlet temperature) 1500 K
α_g	(Gas absorption coefficient) 0.35 m^{-1}
h_m	(Heat transfer coefficient at the heat extraction wall : furnace side) $0.68 \text{ W}/(\text{m}^2\text{K})$
h_r	(Heat transfer coefficient at the heat extraction wall : reacting pipe side) $113 \text{ W}/(\text{m}^2\text{K})$
h_p	(Heat transfer coefficient between the porous medium and the gas) $71 \text{ W}/(\text{m}^2\text{K})$

h_{fw}	(Heat transfer coefficient between the insulated wall and the gas) $36 \text{ W}/(\text{m}^2\text{K})$
$n_p A_p$	(Surface to volume ratio of the porous medium) $1000 \text{ m}^2/\text{m}^3$
τ_e	(Optical thickness of the porous medium) 8
A	(Preexponential constant) $3.3 \times 10^{-4} \text{ s}^{-1}$
E	(Activation energy) 60 kJ/mol
T_r	(Reacting gas inlet temperature) 500 K
h_0	(Heat of combustion of the reacting gas) 1905 kJ/kg

A relative convergence criterion of 10^{-4} was specified in the iterative computation of the temperature and the mole fraction of the product.

4. RESULTS AND DISCUSSION

4.1 Heat transfer analysis for nonparticipating medium

When the working gas is considered as a nonparticipating medium, the equation which shows the radiative exchange between structural walls could be analytically integrated along the z and y direction. The calculated

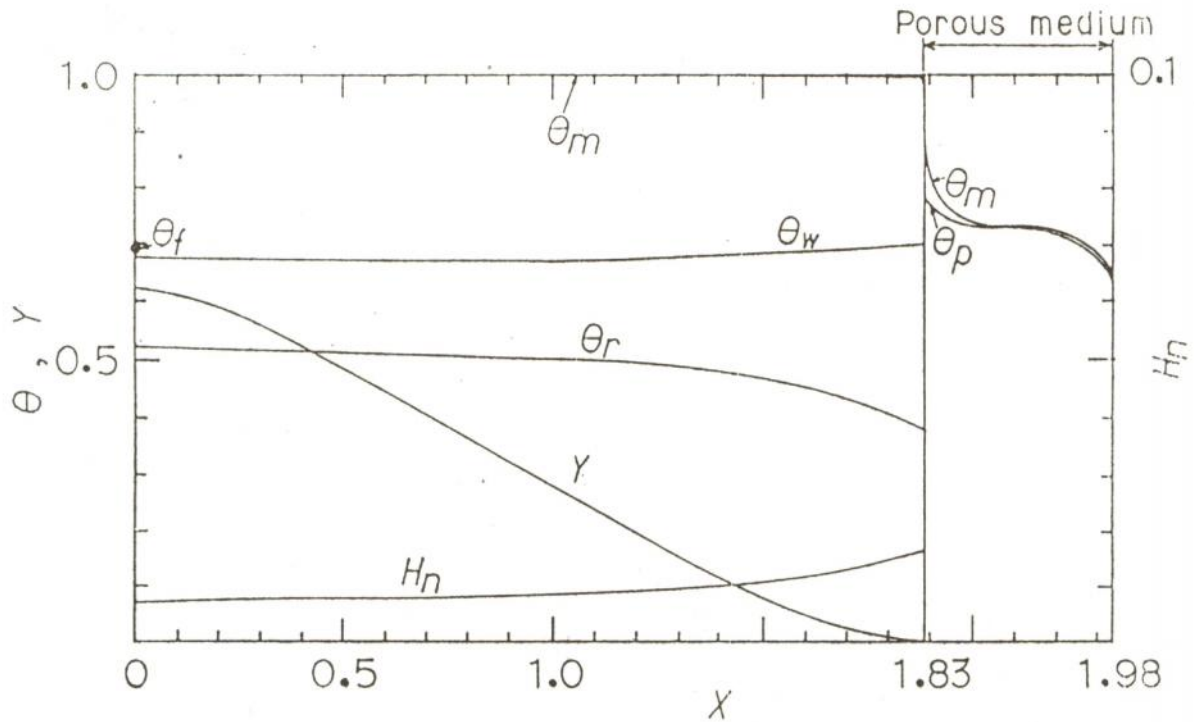


Fig. 5 Temperature distributions, mole fraction of product and net radiative heat flux for nonparticipating medium system.
 $(\chi_g = 0, Re = 890, Re_r = 340)$

results are shown in Fig. 5. In the figure, Θ_f , Θ_m , Θ_w , Θ_p , Θ_r , H_n and Y , respectively, represent floor temperature, combustion gas temperature, heat extraction wall temperature, porous medium temperature, gas temperature in the reacting pipe, net radiative heat flux at the heat extraction wall and mole fraction of the product. The illustrated temperatures are nondimensionalized by the gas temperature at the inlet of the furnace. For better visualization of the temperature distribution in the porous medium, the geometric length of the porous medium is four times magnified along the x axis. The Reynolds number at the inlet of the furnace and at the inlet of the reacting pipe are $Re (= u_m y_e / \nu) = 890$ and $Re_r (= u_r y_r / \nu) = 340$, respectively. As high temperature gas enters the furnace and flows towards the porous medium, its temperature is slightly decreased due to forced convective heat transfer between the gas and the heat extraction wall. When the gas flows into the porous medium, its temperature suddenly decreases because the porous medium effectively converts the enthalpy of the hot gas to thermal radiation. This thermal radiation is mainly

emitted to the upstream direction and is absorbed by the heat extraction wall. However, the distribution of the net radiative heat flux H_n becomes larger as it comes close to the porous medium. Because of this thermal radiation, temperature of the gas flowing inside the reacting pipe Θ_r and mole fraction of the product Y increase along the flow direction (negative x direction).

Figure 6 shows comparison between results of the insulated wall and results of the porous medium. The results of the porous medium are the same as those in Fig. 5. It can be clearly seen that Θ_w , Θ_r and Y of the insulated wall are relatively low when compared with those of the porous medium. This indicates that the heat transfer characteristics of the system with the insulated wall is inferior to those of the system with the porous medium. Hence, for the case of considering the high temperature gas as a nonparticipating medium, the difference between using the porous medium and the insulated wall is prominently proved.

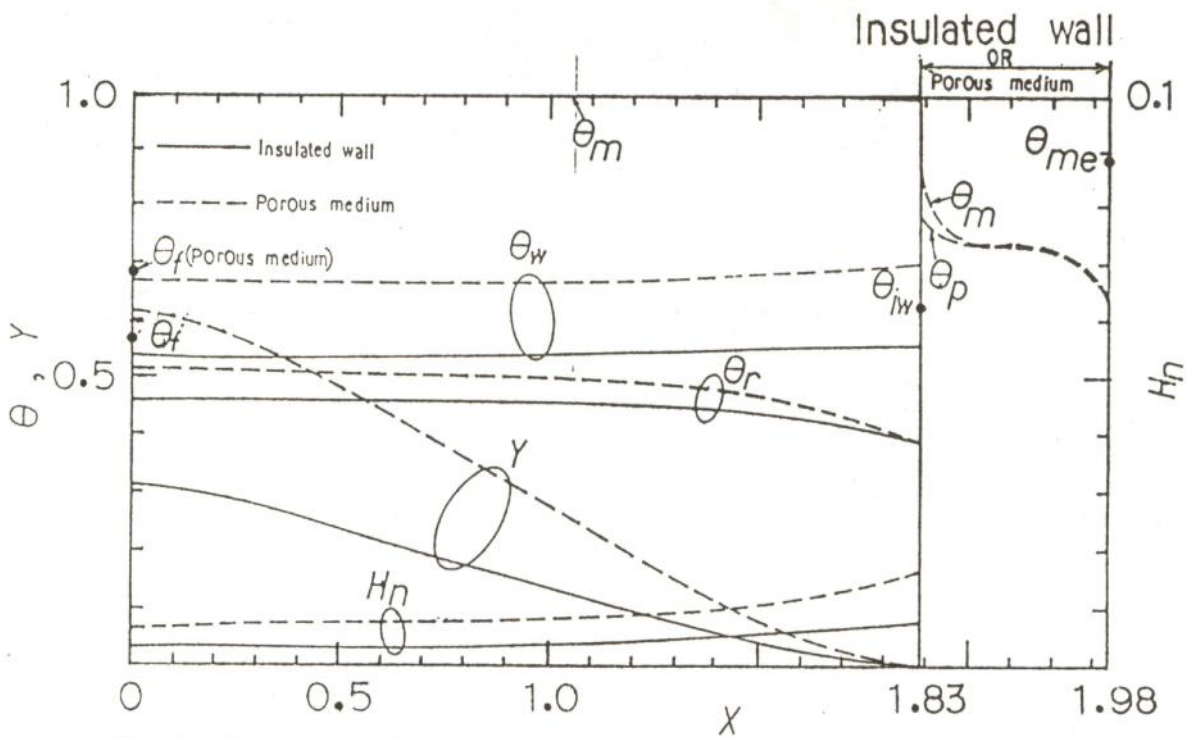


Fig. 6 Comparison between porous medium and insulated wall for nonparticipating medium system.
 $(\alpha_g = 0, Re = 890, Re_r = 340)$

4.2 Heat transfer analysis for participating medium

4.2.1 Heat transfer analysis by gas lump model

A simple method in considering gas radiation is a gas lump model. In this study, the insulated wall is installed at the down-

stream end and the heat transfer analysis in the furnace was conducted by using the gas lump model. The gas lump temperature is an arithmetic mean value between inlet and outlet temperatures of the furnace. The outlet temperature θ_{me} is determined on condition

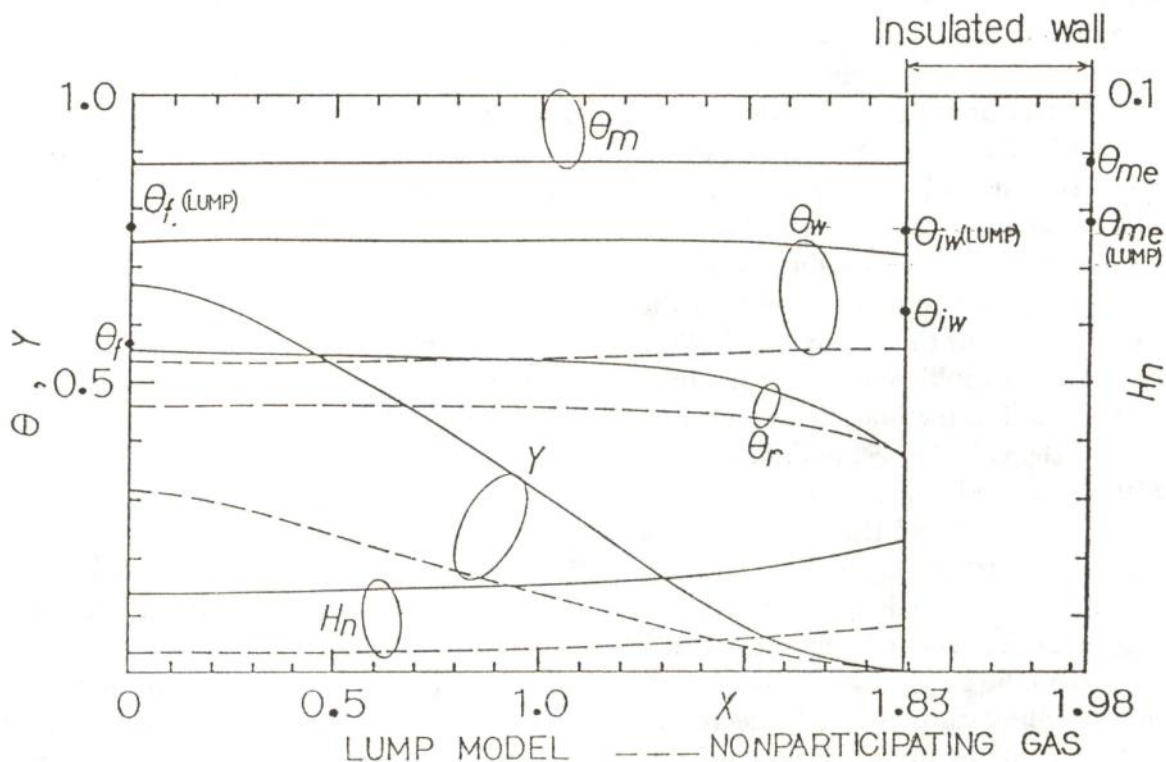


Fig. 7 Comparison between participating medium (lump model) and nonparticipating medium system.
 $(\alpha_g = 0.35 \text{ m}^{-1}, Re = 890, Re_r = 340)$

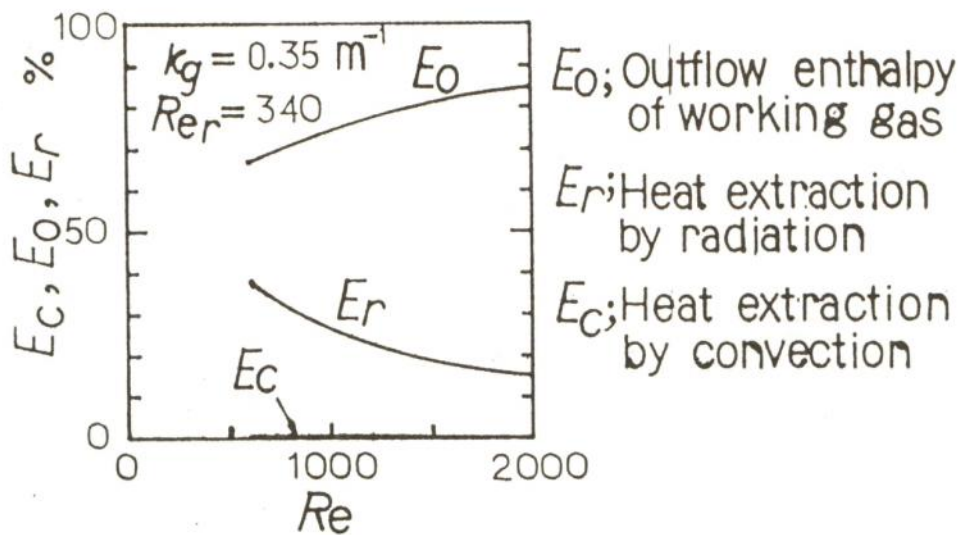


Fig. 8 Overall energy balance for participating medium (lump model).

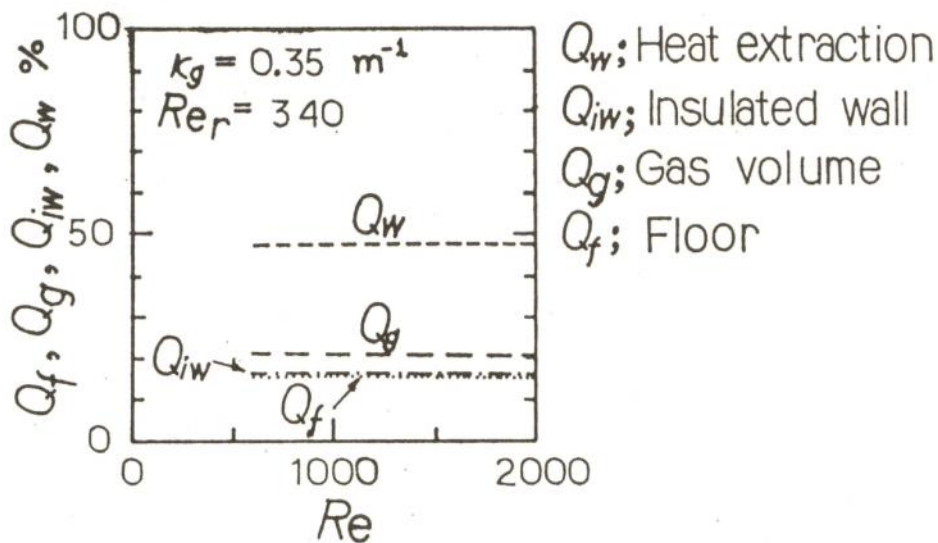


Fig. 9 Contribution of radiative energy from each emitter to the heat extraction wall as a function of Re (lump model).

that the overall energy balance of the system is maintained. Moreover, the computation of the radiative heat transfer between furnace walls is performed by using shape factors in which radiative heat absorption by the gas lump is taken into consideration. Figure 7 shows a typical calculated results of the gas lump model in comparison with those of the nonparticipating gas as shown in Fig. 6 (insulated wall). Here, the absorption coefficient of the gas is 0.35 m^{-1} . It is clearly seen that, for the gas lump model, the heat extraction wall temperature Θ_w , the reacting gas temperature Θ_r as well as the mole fraction of the product at the outlet Y drastically increase due to the radiative energy emitted from the high temperature gas. The corresponding overall

energy balance of the system at various Reynolds number of the furnace is illustrated in Fig. 8. It is clearly understood that the heat transferred by forced convection E_c is extremely small and the radiation E_r is mainly responsible for the heat transfer to the heat extraction wall. Figure 9 exhibits a contribution of radiative energy transferred to the heat extraction wall from emitting body or walls (gas lump Q_g , insulated wall Q_{iw} , furnace floor Q_f and heat extraction wall (opposite wall) Q_w). From the figure, the radiative energy transferred from the opposite wall accounts for about 50% whereas those from the furnace floor, the insulated wall and the gas lump, respectively, are approximately 15-20% irrespective of the Reynolds numbers.

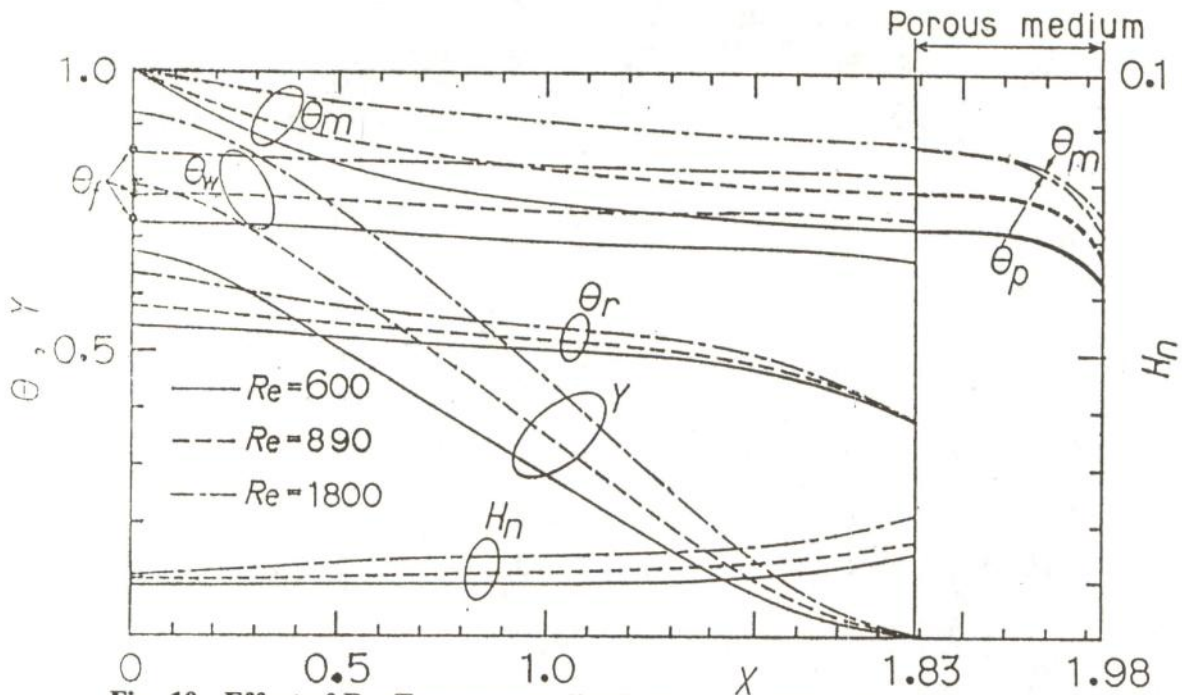


Fig. 10 Effect of Re . Temperature distributions, mold fraction of product and net radiative heat flux for participating medium system by quasi-multi-dimensional model.

($\kappa_g = 0.35 \text{ m}^{-1}$, $Re_r = 340$)

4.2.2. Heat transfer analysis by quasi-multi-dimensional model

Heat transfer analysis in the furnace was performed by using the analytical method as described in section 3.3. Figure 10 shows distributions of temperatures, radiative heat

flux on the heat extraction wall and mole fraction of product against the variation in Reynolds number. As the high temperature participating gas enters the furnace floor and flows towards the porous medium, its temperature considerably decreases due to the

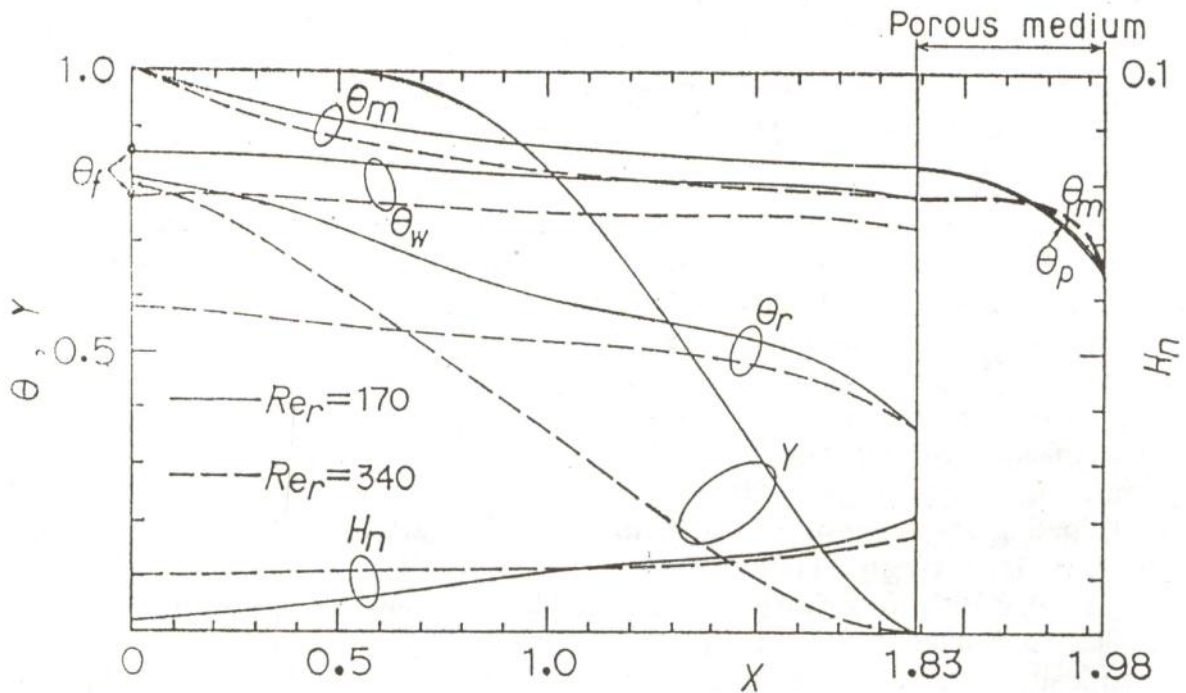


Fig. 11 Effect of Re_r . Temperature distributions, mole fraction of product and net radiative heat flux for participating medium system by quasi-multi-dimensional model.

($\kappa_g = 0.35 \text{ m}^{-1}$, $Re = 890$)

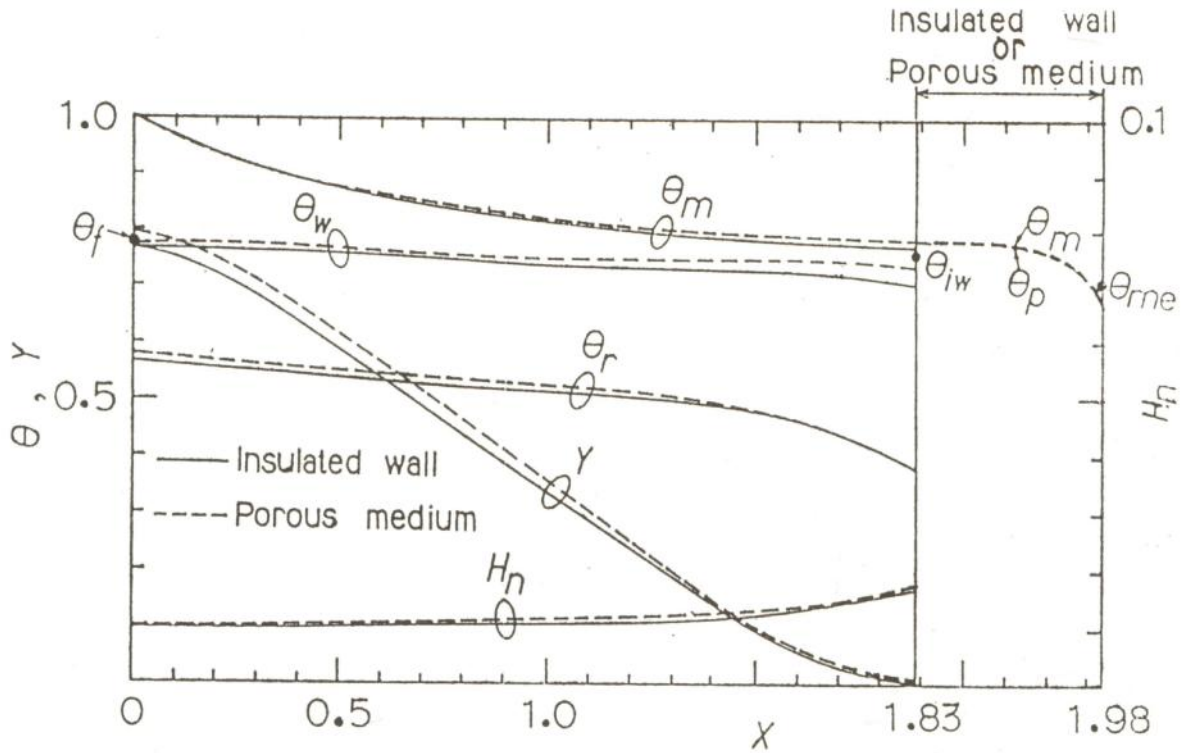


Fig. 12 Comparison between porous medium and insulated wall for participating medium system by quasi-multi-dimensional model.
 $(\kappa_g = 0.35 \text{ m}^{-1}, \text{Re} = 890, \text{Re}_r = 340)$

radiative heat transfer from the gas to the walls of the furnace. The decrease in the gas temperature become prominent as the Reynolds number decreases. On the other hand, for the case of high Reynolds number and high temperature of the gas and the porous medium, the mole fraction of product inside the reacting pipe substantially increases. As an alternative, the production rate of Y can also be increased by decreasing the Reynolds number of the reaction gas, Re_r as shown in Fig. 11. For $\text{Re}_r = 170$, the reaction is completed at a distance three-fourth of the flow path from the inlet of the reacting pipe. Beyond this distance, the radiative energy supplied to the produced gas is merely used in increasing its enthalpy. This results in a decrease in the net radiative heat flux, whereas the reacting gas temperature increases in comparison with that of $\text{Re}_r = 340$. Figure 12 shows comparison between results of the porous medium and results of the insulated wall for the participating gas system. Both of the porous medium and the insulated wall yield almost equal values of temperatures, net radiative heat flux and mole fraction of the product.

This could be understood that the porous medium plays an important role in insulating heat like an insulated wall.

Figures 13 and 14 show overall energy balance of the system and the contribution of radiative energy from each radiating wall and gas volume to the heat extraction wall, respectively, against the variation in Reynolds number, whereas those shown in Fig. 15 and 16 are against the variation in absorption coefficient of the combustion gas. In Fig. 13, even though the magnitude of radiative energy entering the heat extraction wall increases as Re increases, the ratio of it to the total amount of heat entering the furnace denoted by E_r decreases. When the radiative energy entering the heat extraction wall is itemized as shown in Fig. 14, it is clearly seen that all the radiative energy are slightly affected by the change in Re . The contribution of radiative energy emitted from the heat extraction wall is the most prominent since the shape factors are large. However, the high temperature level maintained at the heat extraction wall is actually due to the radiative energy emitted

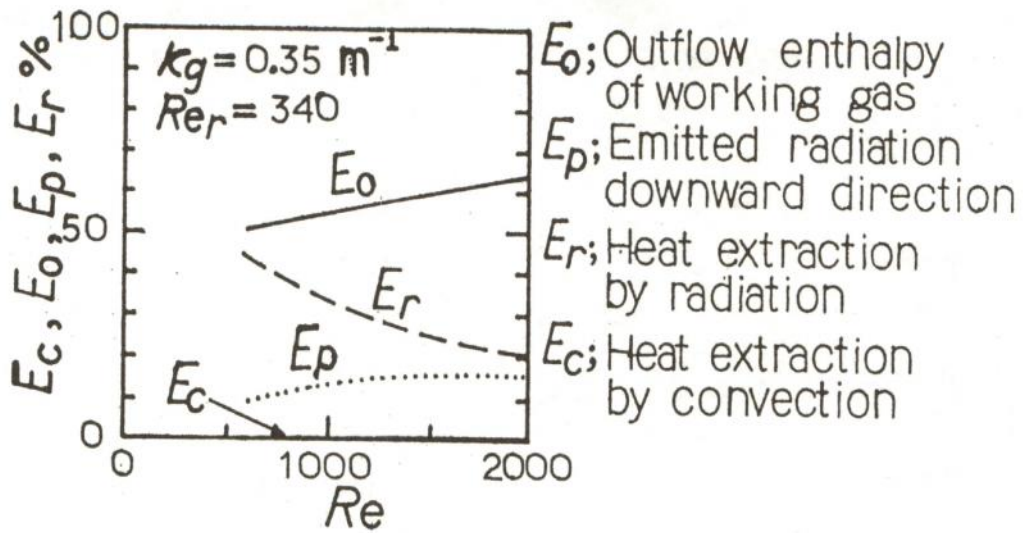


Fig. 13 Overall energy balance as a function of Re for participating medium (quasi-multi-dimensional model).

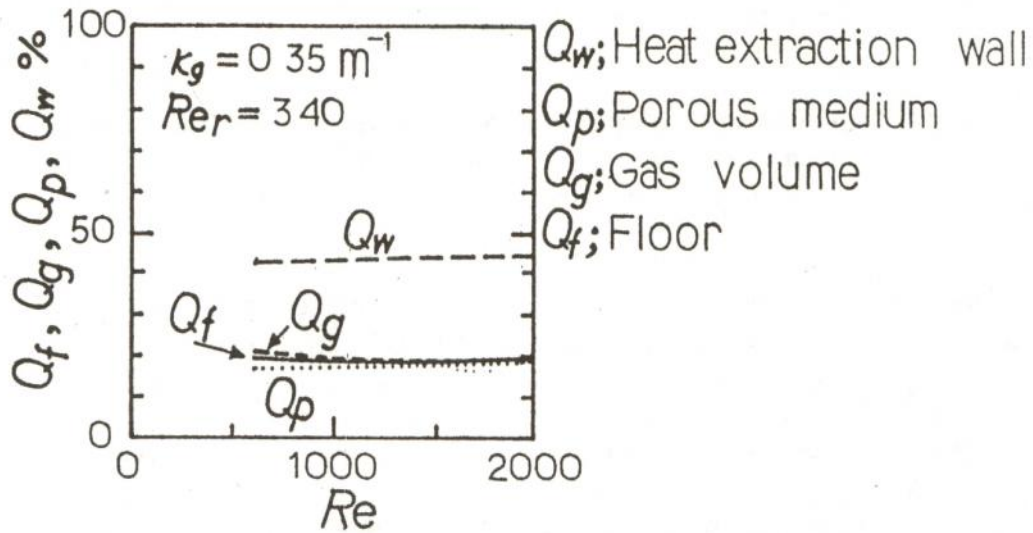


Fig. 14 Contribution of radiative energy from each emitter to the heat extraction wall as a function of Re (quasi-multi-dimensional model).

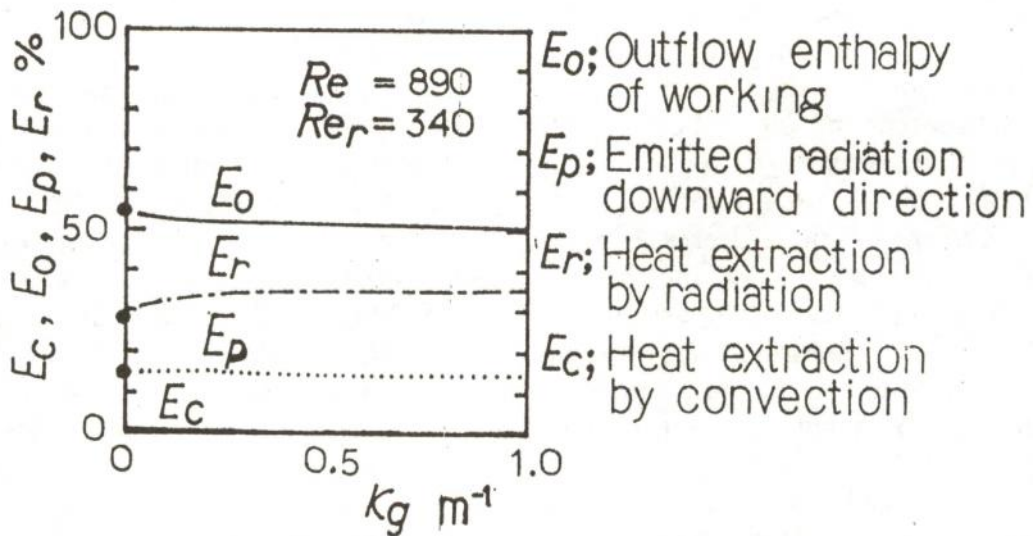


Fig. 15 Overall energy balance as a function of κ_g for participating medium (quasi-multi-dimensional model).

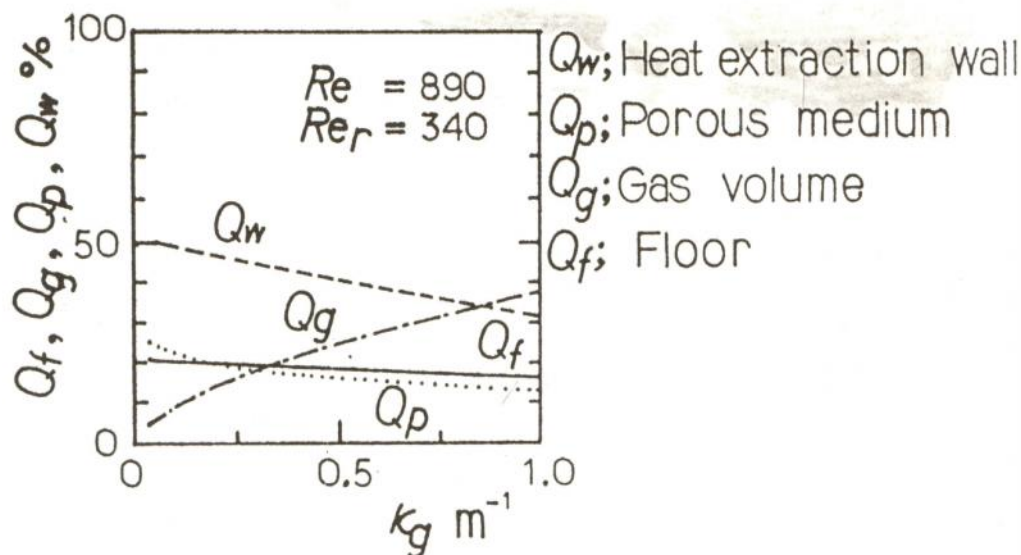


Fig. 16 Contribution of radiative energy from each emitter to the heat extraction wall as a function of κ_g (quasi-multi-dimensional model).

from both the gas and the porous medium. On the other hand, E_r as shown in Fig. 15 increases as the gas absorption coefficient increases. However, the effective enhancement due to the gas radiation is virtually small. Namely, as the radiating gas which flows from a negative x direction at an indefinite distance and enters the furnace at the inlet ($x=0$), it experiences a reduction in its temperature and at the same time provides an incidence radiation for the furnace. However, in this report, even though the gas is considered as a participating medium the inlet temperature is still kept constant ($\Theta = 1$) in the computation. As a result, the calculated gas temperatures near the furnace floor is over estimated. Due to this over estimation of the gas temperature, the substantial increases in the radiation from the gas volume to the heat extraction wall accompanied by a decrease in Q_w , Q_p and Q_f as κ_g increases is natural as shown in Fig. 16. Therefore, it may be reasonable to conclude that the radiative energy which incident upon the heat extraction wall become nearly constant and irrespective of the changes in the absorption coefficient. It is very difficult to provide a suitable method for predicting the overestimation of the calculated radiative energy in this system. However, the comparison of the present heat

transfer analysis method (Fig. 13, 14) and the gas lump model (Fig. 8, 9) shows almost the same results being obtained. This indicates that a relatively good approximation can be achieved by employing the gas lump model.

4.3 Comparison of computed and experimental results

In order to confirm the validity of the proposed numerical method, the computed results are compared with experimental ones with a limited experimental conditions as shown in Fig. 17. Dark lines, represent the computed results, whereas dark circles represent the experimental data. Here, the gas temperature at the inlet is assumed to be equal to the theoretical flame temperature (1800 K). The absorption coefficient of the gas, κ_g is estimated to be 0.35 m^{-1} from the knowledge of the composition and the theoretical flame temperature of the combustion gas. From the consideration of the configuration of the burners used in the experiment, it is very difficult to obtain a uniform velocity distribution and a one dimensional temperature distribution along the flow direction. However, with the power of the proposed analytical method in this study, it is clearly understood that the experimental results are well comparable to the calculated ones.

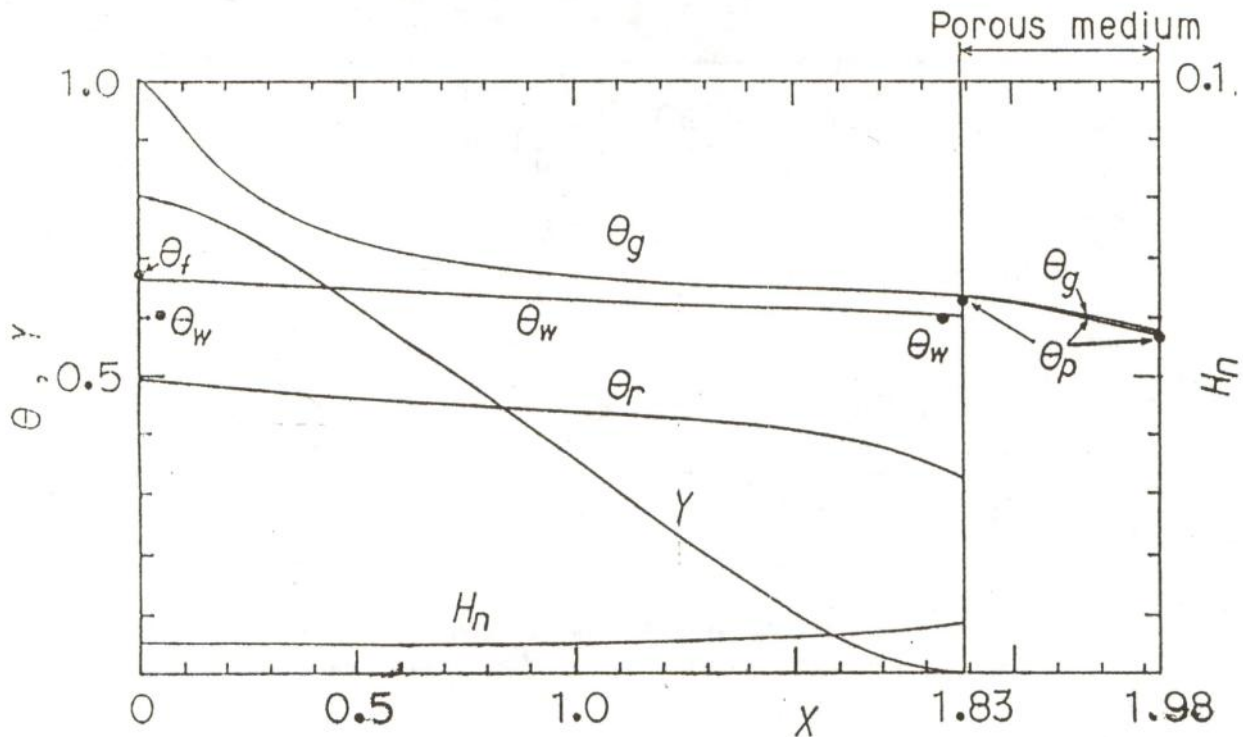


Fig. 17 Comparison between experimental and theoretical result (quasi-multi-dimensional model).

($\kappa_g = 0.35 \text{ m}^{-1}$, $\text{Re} = 423$, $\text{Re}_r = 340$)

5. CONCLUSIONS

The mathematical model of a tubular methane-steam reformer with a convection-radiation converter presented in this paper provides an efficient method of identifying the effect of design and operating parameters on the reformer performance. These findings should be qualified by mentioning that the results are based on a particular reformer design and operating condition. In addition, the calculations were performed on the gray basis for the radiation properties of gases and porous medium. The major conclusions are summarized as follows:

1. The reformer efficiency becomes large if the reformer is equipped with the porous medium rather than the insulated wall for the nonparticipating gas system. However, for the participating gas system, both the porous medium and the insulated wall yield nearly equal reformer efficiency.

2. The reformer efficiency is substantially increased by taking the gas radiation into consideration. This indicates that the gas radiation can not be neglected in the computation and its contribution accounts for about

21 % of the total heat transferred to the heat extraction wall.

3. Radiation is a dominant mode of heat transfer to the heat extraction wall. The convective heat transferred to the wall is negligibly small when compared with radiation.

4. Increasing the flow velocity of the combustion gas increases the reformer efficiency even though the ratio of the heat extraction by radiation at the heat extraction wall decreases. However, the components of the heat extraction by radiation at the wall are almost not affected by the change in flow velocity of the combustion gas. The reformer efficiency can be more effectively increased by decreasing the flow velocity of the reacting gas.

5. The increase in the gas absorption coefficient insignificantly increases the reformer efficiency since the increase in radiative energy emitted from the gas volume is accompanied by the decrease in the radiative energy transferred from the other walls to the heat extraction wall.

6. This system model of a tubular methane-steam reformer with a porous medium by a proposed quasi-multi-dimensio-

nal method showed its usefulness in facilitating the design of a new reformer or in optimizing the operating parameters of an existing reformer.

NOMENCLATURE

A	Preexponential constant, s^{-1}
A_p	surface area of an equivalent sphere, m^2
C_p	gas specific heat at constant pressure, $J/(kg.K)$
E	activation energy, $kJ/mole$
E_n	exponential integral function $= \int_0^1 \mu^{n-2} \exp(-\tau/\mu) d\mu$
H_n	nondimensionalized radiative heat flux at the heat extraction wall
h	heat transfer coefficient, $W/(m^2.K)$
h_0	heat of combustion of the reacting gas, J/kg .
I_e	incidence radiation, W/m^2
n_p	number density of the equivalent sphere, m^{-3}
q_r	radiative heat flux, W/m^2
q_n	net radiative heat flux at the heat extraction wall, W/m^2
Re	Reynolds number
S_1-S_5	optical path length, m
T	temperature, K
u	velocity, m/s
X_e	furnace length, m
Y_e	width of the furnace, m
Y_r	width of the reacting pipe, m
x, y, z	coordinate of the system, m
Y	mole fraction of product in the reacting pipe

GREEK CHARACTERS

Θ	nondimensionalized temperature
χ_g	gas absorption coefficient, m^{-1}
λ	conductivity, $W/(m.K)$
ρ	density, kg/m^3
σ	Stefan-Boltzman constant, $W/(m^2, k^4)$
τ	optical thickness

SUBSCRIPTS

b	black body
e	outlet
f	furnace floor
iw	insulated wall
m	averaged along the y direction
o	inlet
p	porous medium
r	reacting gas in the reacting pipe
w	heat extraction wall

REFERENCES

1. Siegel, R. and Howell, J.R., Thermal Radiation Heat Transfer, 2nd ed. Hemisphere, New York, 1981.
2. Yoshizawa, Y., Echigo, R., Suzuki, H. and Jugjai, S., Combustion Augmentation of Poorly Combustible Materials with High Water Contents. Trans. Japan Soc. Mech. Eng., 1987, 53, 2603. (in Japanese)
3. Yoshizawa, Y., Echigo, R., Jugjai, S. and Komuro, T., Combustion Augmentation of Poorly Combustible Liquid by Porous Medium Energy Converter. Trans. Japan Soc. Mech. Eng., 1988, 54, 3252. (in Japanese)
4. Jugjai, S., Echigo, R., Hanamura, K. and Yoshida, E., Analytical study on the Counterflow Spray Combustion in Radiation Dominated Heat Transfer. Proc. 66th Trans. Japan Soc. Mech. Eng. Conf. Kansai University, 1990, 182-184. (in Japanese)
5. Echigo, R., Effective Energy Conversion Method between Gas Enthalpy and Thermal Radiation and Application to Industrial Furnace. Proc. 7th Int. Heat Transfer Conf., Munich, 1982, 6, 361-366.